Dependence of acceptor levels and hole mobility on acceptor density and temperature in Al-doped *p*-type 4H-SiC epilayers

Hideharu Matsuura,[a] Masahiko Komeda, Sou Kagamihara, Hirofumi Iwata, and Ryohei Ishihara
Department of Electronic Engineering and Computer Science, Osaka Electro-Communication University, 18-8 Hatsu-cho, Neyagawa, Osaka 572-8530, Japan

Tetsuo Hatakeyama, Takatoshi Watanabe, Kazutoshi Kojima, and Takashi Shinohe
Corporate Research & Development Center, Toshiba Corporation, 1 Komukai Toshiba-cho, Saiwai-ku, Kawasaki, Kanagawa 212-8582, Japan

Kazuo Arai
Power Electronics Research Center, National Institute of Advanced Industrial Science and Technology, Tsukuba Center 2, 1-1-1 Umezono, Tsukuba, Ibaraki 305-8568, Japan

(Received 22 April 2004; accepted 2 June 2004)

The temperature-dependent hole concentration $p(T)$ and hole mobility $\mu_p(T)$ are obtained in *p*-type 4H-SiC epilayers with several Al-doping densities. From $p(T)$, the densities and energy levels of acceptors are determined by the graphical peak analysis method (free carrier concentration spectroscopy: FCCS) without any assumptions regarding the acceptor species. In the heavily Al-doped case, the excited states of acceptors affect $p(T)$ because the Fermi level is located between the valence band maximum and the acceptor level (i.e., the ground state level of the acceptor), indicating that a distribution function for acceptors, which includes the influence of excited states of acceptors, should be required. Here, FCCS can determine acceptor densities and acceptor levels using any distribution function (e.g., the Fermi-Dirac distributing function or the distribution function including the influence of excited states). Two types of acceptor species are detected in the lightly Al-doped epilayers, while only one type of acceptor species is found in the heavily Al-doped epilayer. Some of the parameters required to simulate electric characteristics of 4H-SiC power electronic devices are obtained; (1) the dependence of each acceptor level on a total acceptor density and (2) the dependence of the hole mobility on temperature and total impurity density. © *2004 American Institute of Physics*. [DOI: 10.1063/1.1775298]

I. INTRODUCTION

Silicon carbide (SiC) is a wide band gap semiconductor with potential for use in high power and high frequency devices capable of operating at elevated temperatures. Since these devices operate in a wide temperature range from start-up temperatures ($\leqslant$30 °C) to steady-operation temperatures ($\geqslant$300 °C), the following relationships are required in order to carry out device simulation for obtaining optimum SiC device structures, that is, the dependence of the carrier concentrations and the mobilities in SiC on temperature and doping density. For example, the Poisson equation plays an important role in calculating the band bending near junctions such as *pn* junctions and metal-oxide-semiconductor structures, and it requires the relationship between a designed dopant density and an ionized dopant density at any temperature.

In order to obtain these dependences, Hall-effect measurements have been conducted. Although these dependences for *n*-type SiC have been investigated by many researchers,[1–3] those for *p*-type SiC are far from complete. This is because the energy level (i.e., ground state level) of substitutional acceptors in *p*-type SiC becomes deep,[4,5] indicating that the excited states of the acceptor influence the temperature dependence of the hole concentration $p(T)$. Moreover, the acceptor levels in other *p*-type wide band gap semiconductors (e.g., GaN and diamond) are reported to be also deep.[6] Instead of the Fermi-Dirac distribution function that does not include the influence of excited states of acceptors, a distribution function suitable for acceptors in these *p*-type wide band gap semiconductors has been proposed and experimentally tested.[7–12] Moreover, this distribution function is found to be appropriate for determining the densities and energy levels of acceptors in *p*-type wide band gap semiconductors for any dopant density from $p(T)$, while the Fermi-Dirac distribution function is elucidated to be applied only to lightly doped samples.[12] In other words, the distribution function including the influence of excited states should be applied when the Fermi level (E_F) is located between the valence band maximum (E_V) and the acceptor level, while both distribution functions can be applied when E_F is far from E_V.

In this paper, in order to obtain some of the parameters required to simulate electric characteristics of 4H-SiC power electronic devices, we report on our investigation of the dependence of acceptor levels and hole mobility on acceptor density and temperature in Al-doped *p*-type 4H-SiC epilayers. In order to determine the densities and energy levels of

[a]Author to whom correspondence should be addressed; electronic mail: matsuura@isc.osakac.ac.jp

acceptors using $p(T)$ without any assumptions regarding the acceptor species, the graphical peak analysis method (free carrier concentration spectroscopy: FCCS)[7–10,13–20] is applied, where FCCS can determine acceptor densities and acceptor levels using any distributing function (e.g., the Fermi-Dirac distribution function or the distribution function including the influence of excited states of acceptors).[7–10,12] This is because before the analysis of $p(T)$ no one can assert how many types of acceptor species are included in these p-type 4H-SiC epilayers, although many researchers assume that only one type of acceptor species is included there.[21]

II. FREE CARRIER CONCENTRATION SPECTROSCOPY

A. Basic concept

Deep level transient spectroscopy,[22] isothermal capacitance transient spectroscopy (ICTS),[23] and some methods[24,25] can uniquely determine the densities and energy levels of traps in semiconductors or insulators, because each peak in the signal corresponds one-to-one to a trap. For example, the ICTS signal is defined as $S(t) \equiv tdC(t)^2/dt$, where $C(t)$ is the transient capacitance after a reverse bias is applied for a pn diode or a Schottky barrier diode. Since $S(t)$ is theoretically described as the sum of $N_i e_i t \exp(-e_i t)$, it has a peak value of $N_i \exp(-1)$ at a peak time of $t_{\text{peak}\,i} = 1/e_i$. Here, N_i and e_i are the density and emission rate of an ith trap. Therefore, the function of $N_i e_i t \exp(-e_i t)$ plays an important role in the ICTS analysis.

In order to analyze $p(T)$, we have introduced the function theoretically described as the sum of $N_{\text{A}i} \exp(-\Delta E_{\text{A}i}/kT)/kT$,[13] where T is the absolute temperature, k is the Boltzmann constant, $N_{\text{A}i}$ and $\Delta E_{\text{A}i}$ are the density and energy level of an ith acceptor species, and $\Delta E_{\text{A}i}$ is measured from E_{V}. The function of $N_{\text{A}i} \exp(-\Delta E_{\text{A}i}/kT)/kT$ has a peak at $T_{\text{peak}\,i} = \Delta E_{\text{A}i}/k$, which does not apply to all acceptor species in the temperature range of the measurement. If you introduce a function in which a peak appears at $T_{\text{peak}\,i} = (\Delta E_{\text{A}i} - E_{\text{ref}})/k$, you can shift the peak temperature to the measurement temperature range by changing the parameter E_{ref}. This indicates that you can determine $N_{\text{A}i}$ and $\Delta E_{\text{A}i}$ in a wide range of acceptor levels even within a limited measurement temperature range. Therefore, the function to be evaluated should be approximately described as the sum of $N_{\text{A}i} \exp[-(\Delta E_{\text{A}i} - E_{\text{ref}})/kT]/kT$. It should be noted that $N_{\text{A}i}$ and $\Delta E_{\text{A}i}$ determined by this method are independent of E_{ref}. In addition, although Hoffmann proposed an interesting graphical peak analysis method,[26,27] we should avoid introducing a differential evaluation of $p(T)$ because the differential of experimental data results in an increase in observational errors.

B. Theoretical considerations

In the following, we assume a p-type semiconductor with n different acceptor species, and a donor density N_{D}. From the charge neutrality condition, $p(T)$ can be expressed as[28]

$$p(T) = \sum_{i=1}^{n} N_{\text{A}i} F(\Delta E_{\text{A}i}) - N_{\text{D}} \tag{1}$$

in the temperature range in which the electron concentration is much less than $p(T)$. Here, $F(\Delta E_{\text{A}i})$ is either distribution function for acceptors; (1) the Fermi-Dirac distribution function, which is given by[28]

$$f_{\text{FD}}(\Delta E_{\text{A}i}) = \frac{1}{1 + g_{\text{A}} \exp\left(- \dfrac{\Delta E_{\text{F}}(T) - \Delta E_{\text{A}i}}{kT} \right)}, \tag{2}$$

where $\Delta E_{\text{F}}(T)$ is the Fermi level measured from E_{V} at T, and g_{A} is the acceptor degeneracy factor of 4, and (2) the distribution function including the influence of excited states of acceptors, which is described as[12]

$$f(\Delta E_{\text{A}i}) = \frac{1}{1 + g_{\text{A}i}(T) \exp\left(- \dfrac{\Delta E_{\text{F}}(T) - \Delta E_{\text{A}i}}{kT} \right)}, \tag{3}$$

where $g_{\text{A}i}(T)$ is here called the effective acceptor degeneracy factor given by[12]

$$g_{\text{A}i}(T) = g_{\text{A}} \left[1 + \sum_{r=2} g_r \exp\left(\frac{\Delta E_r - \Delta E_{\text{A}i}}{kT} \right) \right] \times \exp\left(- \frac{\overline{E_{\text{exi}}(T)}}{kT} \right), \tag{4}$$

ΔE_r is the difference in energy between E_{V} and the $(r-1)$th excited state level described as[29–31]

$$\Delta E_r = \frac{q^4 m_{\text{p}}^*}{8h^2 \epsilon_{\text{s}}^2 \epsilon_0^2 r^2} = 13.6 \frac{m_{\text{p}}^*}{m_0 \epsilon_{\text{s}}^2 r^2} (\text{eV}), \tag{5}$$

$\overline{E_{\text{exi}}(T)}$ is an ensemble average of the ground $(r=1)$ and excited state $(r \geqslant 2)$ levels of the acceptor measured from $E_{\text{A}i}$, which is expressed as[7–10,12,32]

$$\overline{E_{\text{exi}}(T)} = \frac{\sum_{r=2} (\Delta E_{\text{A}i} - \Delta E_r) g_r \exp\left(- \dfrac{\Delta E_{\text{A}i} - \Delta E_r}{kT} \right)}{1 + \sum_{r=2} g_r \exp\left(- \dfrac{\Delta E_{\text{A}i} - \Delta E_r}{kT} \right)}, \tag{6}$$

where g_r is the $(r-1)$th excited state degeneracy factor of r^2,[29,33] q is the electron charge, m_0 is the free space electron mass, m_{p}^* is the hole effective mass for 4H-SiC, h is Planck's constant, ϵ_0 is the free space permittivity, and ϵ_{s} is the dielectric constant for 4H-SiC. Since the Bohr radius a^* of the ground state is very small, $\Delta E_{\text{A}i}$ is larger than ΔE_1 due to central cell corrections.[34] Since the wave function extension of the $(r-1)$th excited state is of order $r^2 a^*$,[30] the excited state levels are assumed not to be affected by central cell corrections.[35]

On the other hand, using the effective density of states $N_{\text{V}}(T)$ in the valence band, $p(T)$ is written as[28]

$$p(T) = N_{\text{V}}(T) \exp\left(- \frac{\Delta E_{\text{F}}(T)}{kT} \right), \tag{7}$$

where

$$N_V(T) = N_{V0} k^{3/2} T^{3/2} \tag{8}$$

and

$$N_{V0} = 2\left(\frac{2\pi m_p^*}{h^2}\right)^{3/2}. \tag{9}$$

From Eqs. (1) and (7), a favorable function to determine N_{Ai} and ΔE_{Ai} can be introduced as follows. The function to be evaluated is defined as

$$H(T,E_{ref}) \equiv \frac{p(T)^2}{(kT)^{5/2}} \exp\left(\frac{E_{ref}}{kT}\right). \tag{10}$$

Substituting Eq. (1) for one of the $p(T)$ in Eq. (10) and substituting Eq. (7) for the other $p(T)$ in Eq. (10) yield

$$H(T,E_{ref}) = \sum_{i=1}^{n} \frac{N_{Ai}}{kT} \exp\left(-\frac{\Delta E_{Ai} - E_{ref}}{kT}\right) I(\Delta E_{Ai}) - \frac{N_D N_{V0}}{kT} \exp\left(\frac{E_{ref} - \Delta E_F(T)}{kT}\right), \tag{11}$$

where

$$I(\Delta E_{Ai}) = N_{V0} \exp\left(\frac{\Delta E_{Ai} - \Delta E_F(T)}{kT}\right) F(\Delta E_{Ai}). \tag{12}$$

The function

$$\frac{N_{Ai}}{kT} \exp\left(-\frac{\Delta E_{Ai} - E_{ref}}{kT}\right) \tag{13}$$

in Eq. (11) has a peak value of $N_{Ai}\exp(-1)/kT_{peak\,i}$ at the peak temperature

$$T_{peak\,i} = \frac{\Delta E_{Ai} - E_{ref}}{k}. \tag{14}$$

As is clear from Eq. (14), E_{ref} can shift the peak of $H(T,E_{ref})$ within the temperature range of the measurement. Although the actual $T_{peak\,i}$ of $H(T,E_{ref})$ is slightly different from $T_{peak\,i}$ calculated by Eq. (14) due to the temperature dependence of $I(\Delta E_{Ai})$, we can easily determine the accurate values of N_{Ai} and ΔE_{Ai} from the peak of the experimental $H(T,E_{ref})$, using a personal computer. The Windows application software for FCCS can be freely downloaded at our web site (http://www.osakac.ac.jp/labs/matsuura/). This software can also evaluate them by using the curve-fitting method or the differential method.

III. EXPERIMENT

Five 16 μm thick p-type 4H-SiC epilayers with different Al-doping densities were grown on n^+-type 4H-SiC(0001) substrates (sample numbers: No. 1–No. 4), and on a vanadium-doped semi-insulating 4H-SiC(0001) substrate (sample number: No.5). The details of the growth conditions were reported in the previous paper.[36] One 10 μm thick p-type 4H-SiC epilayer on an n^+-type 4H-SiC(0001) substrate (sample number: No. 6) was purchased from Cree Res. Inc. Another 16 μm thick p-type 4H-SiC epilayer was grown on an n^+-type 4H-SiC(11$\bar{2}$0) substrate (sample number: No. 7). They were cut into a $3\times3\text{mm}^2$ size. In order to form good Ohmic contacts at the four corners of the surface of the sample, Al ions were implanted and then ohmic metal (Ni) was deposited. After that, the sample was annealed at 1000 °C in a N_2 atmosphere. $n(T)$ and the temperature dependence of the hole mobility $\mu_p(T)$ were obtained from Hall-effect measurements in van der Pauw configuration using a modified MMR Technologies' Hall system.

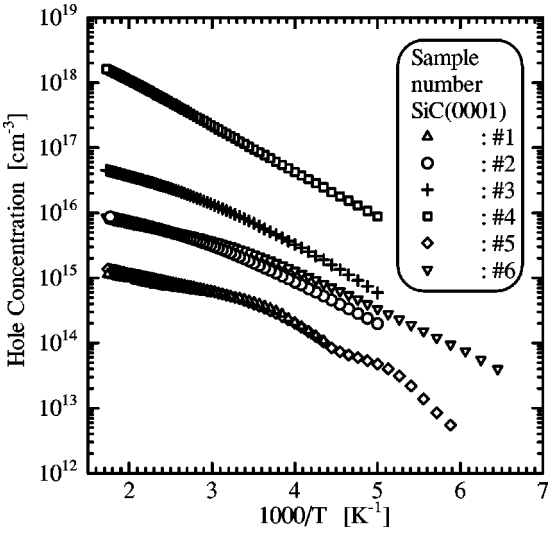

FIG. 1. Temperature dependence of hole concentration.

IV. RESULTS AND DISCUSSION

A. Determination of acceptor levels and acceptor densities

Figure 1 shows $p(T)$ for six samples (triangles: No. 1, circles: No. 2, crosses: No. 3, square: No. 4, diamonds: No. 5, down triangles: No. 6). Figure 2 depicts $\Delta E_F(T)$ for six samples (triangles: No. 1, circles: No. 2, crosses: No. 3, square: No. 4, diamonds: No. 5, down triangles: No. 6), which are calculated by[28]

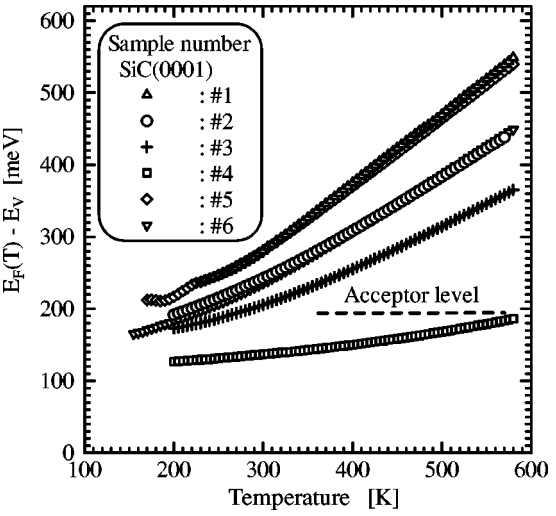

FIG. 2. Temperature dependence of Fermi level.

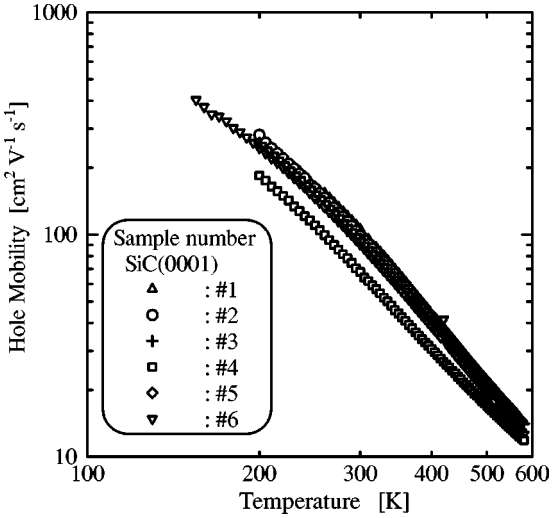

FIG. 3. Temperature dependence of hole mobility.

$$\Delta E_F(T) = kT \ln\left[\frac{N_V(T)}{p(T)}\right]. \tag{15}$$

Since the Al acceptor level in 4H-SiC is reported to be ~200 meV,[4,37] $\Delta E_F(T)$ for samples (No. 1–No. 3, No. 5, No. 6) are higher than this acceptor level at almost all temperatures, while $\Delta E_F(T)$ for No. 4 is lower at all temperatures. According to literature,[7–12] therefore, the $p(T)$ for No. 5 should be analyzed by using $f(\Delta E_A)$, although the $p(T)$ for the others can be analyzed by using either $f_{FD}(\Delta E_A)$ or $f(\Delta E_A)$.

Figure 3 shows $\mu_p(T)$ for six samples (triangles: No. 1, circles: No. 2, crosses: No. 3, square: No. 4, diamonds: No. 5, down triangles: No. 6). Judging from the magnitude of $\mu_p(T)$, the band conduction of holes is dominant over the measurement temperature range. Therefore, $p(T)$ obtained from the Hall-effect measurement is the hole concentration in the valence band.

Using FCCS, the densities and energy levels of acceptors are determined from $p(T)$. Figure 4 shows $H(T,E_{ref})$ with $E_{ref}=8.5\times10^{-3}$ eV for No. 2, which is calculated by Eq. (10). The peak temperature and peak value of $H(T,0.0085)$ are 507.8 K and 1.70×10^{35} cm^{-6} eV$^{-2.5}$. From this peak, the energy level ΔE_{A2} and density N_{A2} of the corresponding acceptor species are determined as 348.7 meV and 4.15×10^{15} cm^{-3}.

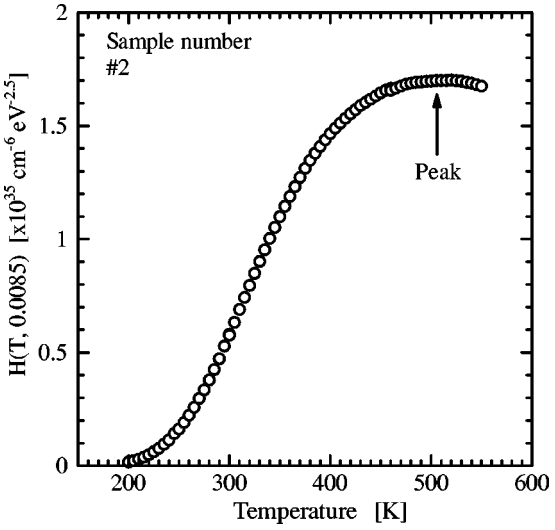

FIG. 4. FCCS signal of $H(T,E_{ref})$ with $E_{ref}=8.5\times10^{-3}$ eV.

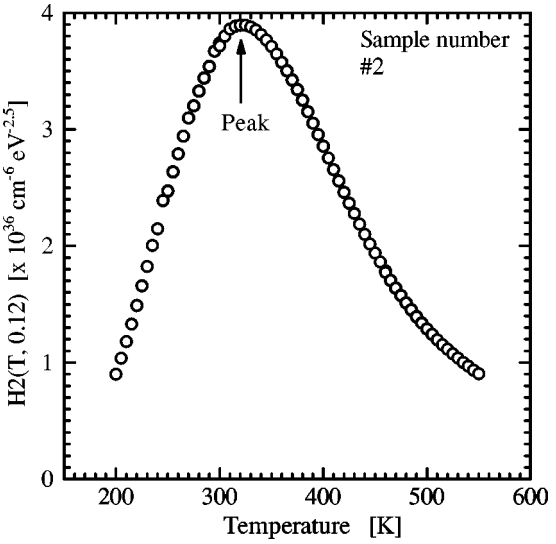

FIG. 5. FCCS signal $H2(T,E_{ref})$ with $E_{ref}=0.12$ eV, in which influence of acceptor species with ΔE_{A2} is removed.

In order to investigate another acceptor species included in this epilayer, the FCCS signal of $H2(T,E_{ref})$, in which the influence of the above-determined donor species is removed, is calculated using the following equation. It is clear from Eq. (11) that

$$H2(T,E_{ref}) = \frac{p(T)^2}{(kT)^{5/2}}\exp\left(\frac{E_{ref}}{kT}\right) - \frac{N_{A2}}{kT}\exp\left(-\frac{\Delta E_{A2}-E_{ref}}{kT}\right)I(\Delta E_{A2}) \tag{16}$$

is not influenced by the acceptor species with ΔE_{A2}. Figure 5 depicts $H2(T,E_{ref})$ with $E_{ref}=0.12$ eV. Since a peak appears in the $H2(T,0.12)$ signal, another acceptor species is in-

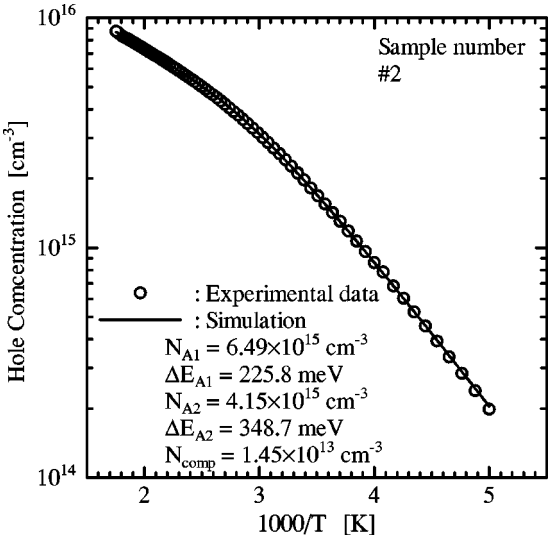

FIG. 6. $p(T)$ simulation.

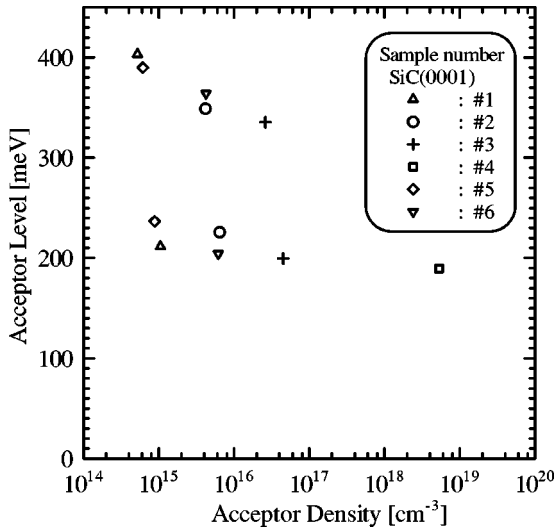

FIG. 7. Results determined by FCCS.

cluded in this epilayer. Using the peak temperature of 323.1 K and the peak value of 3.89×10^{36} cm^{-6} eV$^{-2.5}$, the acceptor level ΔE_{A1} and density N_{A1} are determined to be 225.8 meV and 6.49×10^{15} cm^{-3}.

The FCCS signal of $H3(T,E_{ref})$, in which the influence of two acceptor species above-determined are removed, is calculated. However, $H3(T,E_{ref})$ is nearly zero, indicating that this epilayer includes only two types of acceptor species. Finally, N_D is determined as 1.45×10^{13} cm^{-3}.

In order to verify the values obtained by FCCS, $p(T)$ is simulated using Eqs. (1) and (7). The open circles in Fig. 6 represent the experimental $p(T)$ and the solid line represents the $p(T)$ simulation. The solid line is in good agreement with the experimental $p(T)$, indicating that the values determined by FCCS are reliable. These values are shown in Fig. 7, denoted by circles.

In the same way as illustrated for No. 2, the acceptor levels and acceptor densities for the others are determined, and are shown in Fig. 7, denoted by triangles for No. 1, crosses for No. 3, squares for No. 4, diamonds for No. 5, and down triangles for No. 6. In the case of the heaviest Al-doped epilayer (No. 4), only one type of acceptor species is detected. It is clear from Fig. 7 that ΔE_{A1} and ΔE_{A2} depend on the acceptor density.

TABLE I. Parameters for acceptor levels in Al-doped 4H-SiC.

$E_{A1}(0)$ (meV)	α_{A1} (meV cm)	$E_{A2}(0)$ (meV)	α_{A2} (meV cm)
220	1.90×10^{-5}	413	2.07×10^{-4}

From photoluminescence (PL) measurements[4] and Hall-effect measurements,[37] the energy level of ~200 meV is ascribed to an isolated, substitutional Al in 4H-SiC, suggesting that the origin of the shallow acceptor level is the Al acceptor. On the other hand, although the possible origin of the deep acceptor level is B with which 4H-SiC is sometimes contaminated, the concentration of B in this epilayer, which was determined by secondary ion mass spectroscopy, was $<4\times10^{14}$ cm^{-3}. Moreover, the B acceptor level was reported to be 285 meV.[37] It may be closely linked with the D_1 line observed by PL (Refs. 38 and 39) or with a complex (Al_{Si}-V_C) (Ref. 40) of Al at a Si site (Al_{Si}) and a carbon vacancy (V_C) just like a reported complex (B_{Si}-V_C) of B at a Si site (B_{Si}) and V_C.[41] From the study on lightly Al-doped 4H-SiC irradiated with 1 MeV electrons, it is reported that N_{A2} is unchanged while N_{A1} reduces.[20] However, the origin of the deep acceptor level is unfortunately unknown to date.

B. Dependence of each acceptor level on total acceptor density

Figure 8 depicts the dependence of the acceptor levels on a total acceptor density ($N_{A,total}\equiv N_{A1}+N_{A2}$). The dependence of each acceptor level on $N_{A,total}$ is investigated here, while the dependence of one dopant level on one dopant density was discussed in Si that included one type of dopant species.[42]

An ideal acceptor level $\Delta E_{Ai}(0)$ is the energy required to emit one hole from the acceptor site into infinity on E_V. However, since a *p*-type semiconductor is electrically neu-

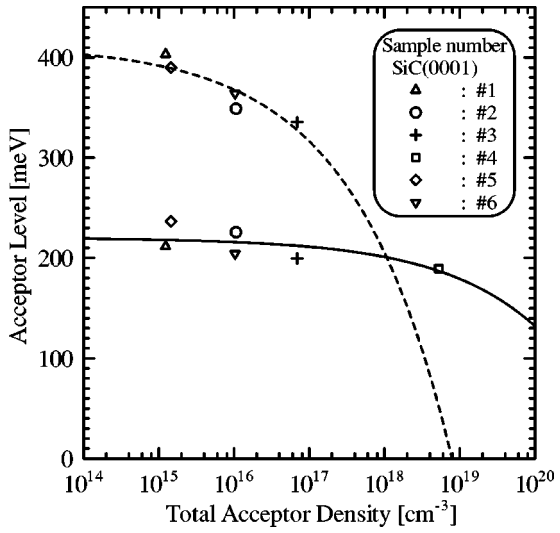

FIG. 8. Dependence of each acceptor level on total acceptor density.

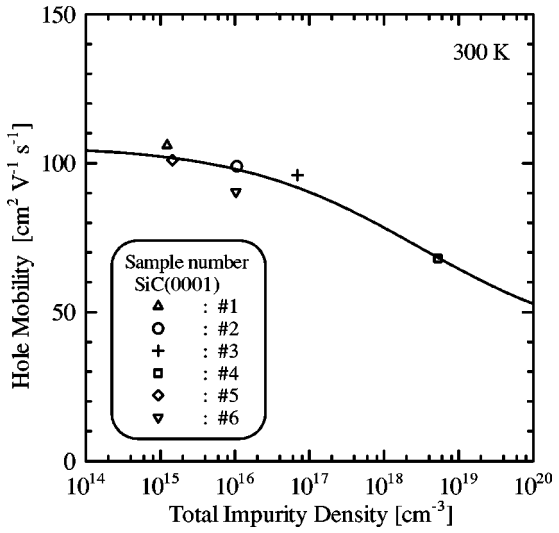

FIG. 9. Dependence of hole mobility on total impurity density.

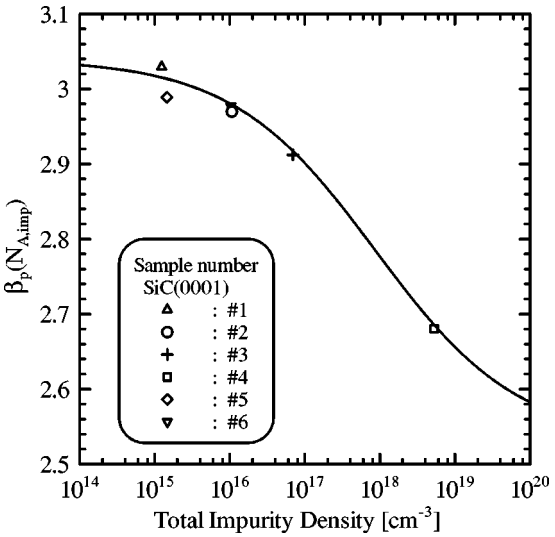

FIG. 10. $\beta_p(N_{A,imp})$ in $\mu_p(T,N_{A,imp}) \propto T^{\beta_p(N_{A,imp})}$.

tral, each negatively charged acceptor is shielded by one hole on E_V. This shielding hole is assumed to be located within half $(\overline{r})$ of an average distance $(1/\sqrt[3]{N_{A,total}})$ of acceptors, indicating that the acceptor level should be lowered by the energy higher than $q/(4\pi\epsilon_s\varepsilon_0\overline{r})$ due to Coulomb's attraction.[43] Therefore,

$$\Delta E_{Ai}(N_{A,total}) = \Delta E_{Ai}(0) - \alpha_{Ai}\sqrt[3]{N_{A,total}} \tag{17}$$

and

$$\alpha_{Ai} \geqslant \frac{q}{8\pi\epsilon_s\epsilon_0} = 2.44\times10^{-5}\ \text{meV cm}. \tag{18}$$

The fitting parameters obtained by a least-squares fit of Eq. (17) to data in Fig. 8 are listed in Table I. The $\Delta E_{A1}(N_{A,total})$ and $\Delta E_{A2}(N_{A,total})$ simulations are denoted by the solid and broken lines in Fig. 8, respectively. Since α_{A1} is close to the value in Eq. (18), the hole goes around the shallow ionized acceptor within a radius of approximately $\overline{r}$. However, the hole rounds more closely on the deep ionized acceptor because of the large α_{A2}.

C. Dependence of hole mobility on temperature and total impurity density

In Fig. 3, $\mu_p(T,N_{A,imp})$ at >250 K can be expressed as

$$\mu_p(T,N_{A,imp}) = \mu_p(300,N_{A,imp})\left(\frac{T}{300}\right)^{-\beta_p(N_{A,imp})}, \tag{19}$$

where $N_{A,imp}=N_{A1}+N_{A2}+N_D$,[44] because all impurities affect the hole mobility. In order to obtain $\mu_p(T,N_{A,imp})$, $\mu_p(300,N_{A,imp})$ and $\beta_p(N_{A,imp})$ we can individually evaluate.

Figure 9 shows $\mu_p(300,N_{A,imp})$ for samples (No. 1–No. 6) corresponding to 4H-SiC(0001) substrates. According to literature,[1,36,45] $\mu_p(300,N_{A,impl})$ can be described as

TABLE II. Parameters for $\mu_p(300,N_{A,imp})$ in Al-doped 4H-SiC.

μ_p^{min} [cm^2/(V s)]	μ_p^{max} [cm^2/(V s)]	N_p^{μ} (cm^{-3})	γ_p^{μ}
37.6	106.0	2.97×10^{18}	0.356

TABLE III. Parameters for β_p $(N_{A,imp})$ in Al-doped 4H-SiC.

β_p^{min}	β_p^{max}	N_p^{β} (cm^{-3})	γ_p^{β}
2.51	3.04	8.64×10^{17}	0.456

$$\mu_p(300,N_{A,imp}) = \mu_p^{min}(300) + \frac{\mu_p^{max}(300) - \mu_p^{min}(300)}{1+\left(\frac{N_{A,imp}}{N_p^{\mu}}\right)^{\gamma_p^{\mu}}}, \tag{20}$$

where $\mu_p^{min}(300)$, $\mu_p^{max}(300)$, N_p^{μ}, and γ_p^{μ} are the fitting parameters. By a least-squares fit of Eq. (20) to $\mu_p(300)$ shown in Fig. 9, these fitting parameters are determined and listed in Table II. The solid line in Fig. 9 represents the $\mu_p(300,N_{A,imp})$ simulation.

Figure 10 shows $\beta_p(N_{A,imp})$ in Eq. (19) for samples (No. 1–No. 6) corresponding to 4H-SiC(0001) substrates. In the same way as illustrated for $\mu_p(T,N_{A,imp})$, the following relationship is assumed:

$$\beta_p(N_{A,imp}) = \beta_p^{min} + \frac{\beta_p^{max} - \beta_p^{min}}{1+\left(\frac{N_{A,imp}}{N_p^{\beta}}\right)^{\gamma_p^{\beta}}}, \tag{21}$$

where β_p^{min}, β_p^{max}, N_p^{β}, and γ_p^{β} are the fitting parameters. By a least-squares fit of Eq. (21) to $\beta_p(N_{A,total})$ shown in Fig. 10, these fitting parameters are determined and listed in Table III. The solid line in Fig. 10 represents the $\beta_p(N_{A,imp})$ simulation.

D. Difference in $p(T)$ and $\mu_p(T)$ between epilayers grown on SiC(0001) and (11$\bar{2}$0) surfaces

Figures 11 and 12 show three $p(T)$ and three $\mu_p(T)$ for epilayers grown on two SiC(0001) surfaces (No. 1, No. 6) and one SiC(11$\bar{2}$0) surface (No. 7). Only in the epilayer (No. 7) grown on the SiC(11$\bar{2}$0) surface, the unusual peak appeared in $p(T)$ at ~400 K, at which the unusual dip occured

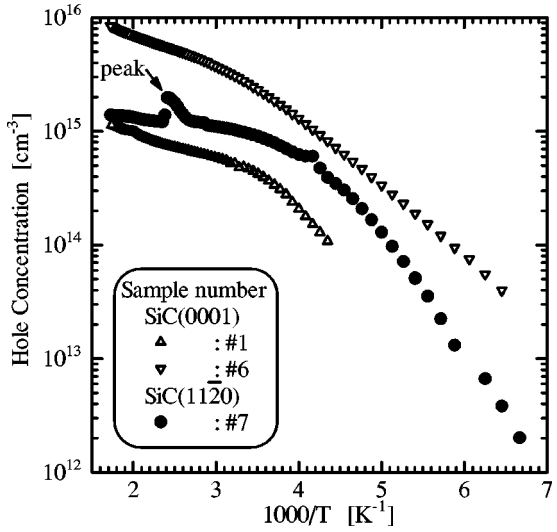

FIG. 11. Dependence of $p(T)$ on crystal orientation of 4H-SiC.

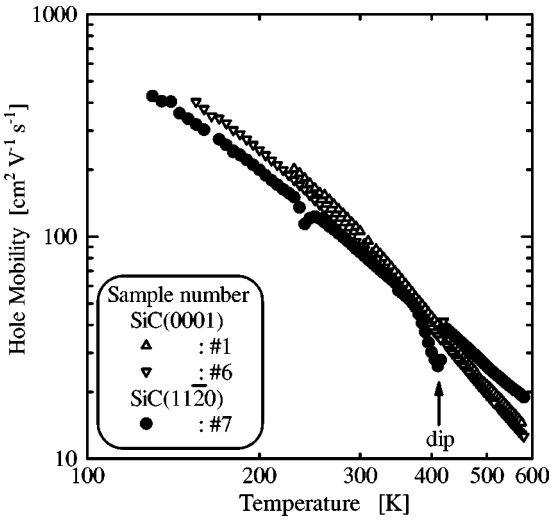

FIG. 12. Dependence of $\mu_p(T)$ on crystal orientation 4H-SiC.

in $\mu_p(T)$. Although several Hall-effect measurements were conducted in this sample from low to high temperature or from high to low temperature, this phenomenon appeared repeatedly. Although similar phenomena are reported in some of *p*-type polycrystalline silicon wafers for solar cells,[46] the origin of these phenomena has not been reported yet.

Using $p(T)$ in which this unusual peak is eliminated, the densities and energy levels are determined by FCCS; $N_{A1}=1.21\times10^{15}$ cm^{-3}, $\Delta E_{A1}=189$ meV, $N_{A2}=2.17\times10^{14}$ cm^{-3}, and $\Delta E_{A2}=374$ meV. Compared with the acceptor levels for epilayers grown on SiC(0001) substrates shown in Fig. 7, the acceptor levels are a little lower. In the case of $\mu_p(T)$, on the other hand, $\beta_p(N_{A,imp})$ for No. 7 is 2.23, which is much lower than those for the epilayers grown on SiC(0001) surfaces. The investigation on the cause of this difference is in progress.

V. CONCLUSION

$p(T)$ and $\mu_p(T)$ for Al-doped 4H-SiC epilayers grown on n^+-type 4H-SiC(0001) substrates were obtained from Hall-effect measurements. From $p(T)$, the densities and energy levels of acceptors were determined by the graphical peak analysis method without any assumptions regarding the acceptor species using the Fermi-Dirac distribution function or the distribution function including the effect of excited states of acceptors. Two types of acceptor species were detected. The shallow acceptor species was ascribed to substitutional Al acceptor species, while the deep one was uncertain. In order to determine some of the parameters required in device simulation, the dependence of each acceptor level on a total acceptor density and the dependence of the hole mobility on temperature and total impurity density were investigated.

ACKNOWLEDGMENTS

This work was partially supported by the Academic Frontier Promotion Projects of the Ministry of Education, Culture, Sports, Science and Technology (MEXT), and it was partially supported by the R&D Association of Future Electron Devices (FED) and the NewEnergy and Industrial Technology Development Organization (NEDO).

[1] W. J. Schaffer, G. H. Negley, K. G. Irvine, and J. W. Palmour, Mater. Res. Soc. Symp. Proc. **339**, 595 (1994).
[2] J. Pernot, S. Contreras, J. Camassel, J. L. Robert, W. Zawadzki, E. Neyret, and L. D. Cioccio, Appl. Phys. Lett. **77**, 4359 (2000).
[3] H. Matsunami and T. Kimoto, Mater. Sci. Eng., R. **20**, 125 (1997).
[4] M. Ikeda, H. Matsunami, and T. Tanaka, Phys. Rev. B **22**, 2842 (1980).
[5] I. Nashiyama, *Properties of Silicon Carbide*, edited by G. L. Harris (INSPEC, London, 1995), p. 87.
[6] O. Madelung, *Semiconductors: Data Handbook*, 3rd ed. (Springer, Berlin, 2004), p. 15 and p. 108.
[7] H. Matsuura, New J. Phys. **4**, 12.1 (2002) [http://www.njp.org/].
[8] H. Matsuura, Mater. Sci. Forum **389–393**, 679 (2002).
[9] H. Matsuura, K. Sugiyama, K. Nishikawa, T. Nagata, and N. Fukunaga, Mater. Sci. Forum **433–436**, 447 (2003).
[10] H. Matsuura, K. Sugiyama, K. Nishikawa, T. Nagata, and N. Fukunaga, J. Appl. Phys. **94**, 2234 (2003).
[11] H. Matsuura *et al.*, Phys. Status Solidi C **0**, 2214 (2003).
[12] H. Matsuura, J. Appl. Phys. **95**, 4213 (2004).
[13] H. Matsuura and K. Sonoi, Jpn. J. Appl. Phys., Part 2 **35**, L555 (1996).
[14] H. Matsuura, Jpn. J. Appl. Phys., Part 1 **36**, 3541 (1997).
[15] H. Matsuura, Y. Uchida, T. Hisamatsu, and S. Matsuda, Jpn. J. Appl. Phys., Part 1 **37**, 6034 (1998).
[16] H. Matsuura, T. Kimoto, and H. Matsunami, Jpn. J. Appl. Phys., Part 1 **38**, 4013 (1999).
[17] H. Matsuura, Y. Uchida, N. Nagai, T. Hisamatsu, T. Aburaya, and S. Matsuda, Appl. Phys. Lett. **76**, 2092 (2000).
[18] H. Matsuura, Y. Masuda, Y. Chen, and S. Nishino, Jpn. J. Appl. Phys., Part 1 **39**, 5069 (2000).
[19] H. Matsuura, K. Morita, K. Nishikawa, T. Mizukoshi, M. Segawa, and W. Susaki, Jpn. J. Appl. Phys., Part 1 **41**, 496 (2002).
[20] H. Matsuura, K. Aso, S. Kagamihara, H. Iwata, T. Ishida, and K. Nishikawa, Appl. Phys. Lett. **83**, 4981 (2003).
[21] F. Schmid, M. Krieger, M. Laube, G. Pensl, and G. Wagner, *Silicon Carbide*, edited by W. J. Choyke, H. Matsunami, and G. Pensl (Springer, Berlin, 2004), pp. 517–536.
[22] D. V. Lang, J. Appl. Phys. **45**, 3023 (1974).
[23] H. Okushi, Philos. Mag. B **52**, 33 (1985).
[24] H. Matsuura, J. Appl. Phys. **64**, 1964 (1988).
[25] H. Matsuura, T. Hase, Y. Sekimoto, M. Uchida, and M. Simizu, J. Appl. Phys. **91**, 2085 (2002).
[26] H. J. Hoffmann, Appl. Phys. **19**, 307 (1979).
[27] H. J. Hoffmann, H. Nakayama, T. Nishino, and H. Hamakawa, Appl. Phys. A: Solids Surf. **33**, 47 (1984).
[28] S. M. Sze, *Physics of Semiconductor Devices*, 2nd ed. (Wiley, New York, 1981), Chap. 1.
[29] P. Y. Yu and M. Cardona, *Fundamentals of Semiconductors: Physics and Materials Properties*, 2nd ed. (Springer, Berlin, 1999), p. 156.
[30] B. Sapoval and C. Hermann, *Physics of Semiconductors* (Springer, New York, 1993), p. 73.
[31] J. Singh, *Semiconductor Devices: An Introduction* (McGraw-Hill, New York, 1994), p. 110.
[32] K. F. Brennan, *The Physics of Semiconductors with Applications to Optoelectronic Devices* (Cambridge University Press, Cambridge, 1999), p. 277.
[33] B. Sapoval and C. Hermann, *Physics of Semiconductors* (Springer, New York , 1993), p. 112.
[34] P. Y. Yu and M. Cardona, *Fundamentals of Semiconductors: Physics and Materials Properties*, 2nd ed. (Springer, Berlin, 1999), p. 160.
[35] P. Y. Yu and M. Cardona, *Fundamentals of Semiconductors: Physics and Materials Properties*, 2nd ed. (Springer, Berlin, 1999), p. 162.
[36] T. Hatakeyama *et al.*, Mater. Sci. Forum **433–436**, 443 (2003).
[37] T. Troffer, M. Schadt, T. Frank, H. Itoh, G. Pensl, J. Heindl, H. P. Strunk, and M. Maier, Phys. Status Solidi A **162**, 277 (1997).

[38]T. Egilsson, J. P. Bergman, I. G. Ivanov, A. Henry, and E. Janzën, Phys. Rev. B **59**, 1956 (1999).
[39]W. J. Choyke and R. P. Devaty, in *Silicon Carbide*, edited by W. J. Choyke, H. Matsunami, and G. Pensl (Springer, Berlin, 2004), p. 423.
[40]I. V. Ilyin, E. N. Mokhov, and P. G. Baranov, Mater. Sci. Forum **353–356**, 521 (2001).
[41]P. G. Baranov, I. V. Ilyin, and E. N. Mokhov, Phys. Solid State **39**, 52 (1997).
[42]G. L. Pearson and J. Bardeen, Phys. Rev. **75**, 865 (1949).
[43]Because of Coulomb's repulsion by positively charged donors, $N_{A,total}$ can be described as $N_{A,total} \simeq \Sigma_i N_{Ai} - N_D$. However, since N_D in the epilayers studied here is much lower than the sum of acceptor densities, N_D is neglected in this article.
[44]Since N_D in the epilayers studied here is much lower than the sum of acceptor densities, the influence of N_D on $p(T)$ is neglected in this article.
[45]D. M. Caughey and R. E. Thomas, Proc. IEEE **55**, 2192 (1967).
[46]H. Matsuura, T. Ishida, K. Nishikawa, N. Fukunaga, and T. Kuroda, Solid State Phenom. **93**, 141 (2003).